Wireless Personal Communications (2023) 133:2105–2124
https://doi.org/10.1007/s11277-023-10831-4

A Novel Radial Kernel Watershed Basis Segmentation Algorithm for Color Image Segmentation

Chandana Kumari[1] · **Abhijit Mustafi**[1]

Accepted: 21 December 2023 / Published online: 20 February 2024
© The Author(s), under exclusive licence to Springer Science+Business Media, LLC, part of Springer Nature 2024

Abstract
Human vision cannot analyze the huge amount of information hidden in color images. Thus, amongst the research being developed currently, Color Image Segmentation (CIS) has become more vital. As each pixel in the image constitutes a different color complexion, which is tedious for estimating, CIS is a challenging process; also, it is a time-consuming process. Hence, this work proposes novel thresholding utilizing the Chaotic Logistic Fertile Field optimization Algorithm (CLFFA) approach and segmentation utilizing the Radial Kernel Watershed Basis Segmentation (RKWBS) technique for reducing time consumption. Utilizing the Contrast Limited Recursive Least Square Histogram Equalization (CLRLSHE) algorithm, the input image's contrast is enriched initially. Then, the Sobel edge detection detects the edges from the preprocessed image. Also, the CLFFA algorithm finds the optimal threshold value. After that, by thresholding the edge detected image grounded on RKWBS, the image is segmented quickly. Lastly, for removing the unwanted information in the segmented image, morphological operations are executed in it. Experiments were executed and analogized with the prevailing frameworks for proving the proposed mechanism's efficacy. The outcomes proved the efficacy regarding segmentation accuracy, computational time, et cetera.

Keywords Contrast Limited Recursive Least Square Histogram Equalization (CLRLSHE) · Chaotic Logistics Fertile Field Algorithm (CLFFA) · Radial Kernel Watershed Basis Segmentation (RKWBS) · Color Image Segmentation · Sobel edge detection

1 Introduction

As the computational complexity is caused by the non-linear operations that are involved in mapping the colors betwixt spaces, image segmentation by color features and textures has become a relatively, recent topic that has been addressed [12]. Segmentation, which is a low-level operation for analyzing the given color image spontaneously, is a significant

✉ Chandana Kumari
chandana.jsr@gmail.com

[1] Department of Computer Science & Engineering, Birla Institute of Technology, Mesra, Ranchi, India

technique in digital image processing along with computer vision [14]. Image segmentation not only distinguishes interesting objects as of the background but also identifies them in an image [18]. Grouping the pixels in an image, which are of the same values, into several meaningful homogeneous regions is done in the image segmentation process [10]. To segment the image, numerous prevailing works have been developed. The region-based system, threshold-based approach, edge-based framework, neural network-based model, et cetera are some of the popular researches [15]. In edge detection-centric segmentation, the pixels present on the edge of an image are founded. Here, the segmentation boundary is generally identified via high gray gradient locations [6]. Sobel operator, canny, Laplace operator, fuzzy logic, and so on are some of the edge detecting tools. The regions are grown corresponding to the neighbouring pixels' similarity with the seed pixel in region-based segmentation. Some region-based segmentation techniques are watershed algorithm, split and merge algorithm, region growing system, and level set algorithm. For segmenting the image in neural network-centric techniques, the neurons in the neural networks are wielded.

The most popular image segmentation processing is grounded on thresholding-centered methodologies. Selecting a set of TVs utilizing several characteristics defined from images is involved in thresholding techniques [21]. Global thresholding, local thresholding, and adaptive thresholding are the three classifications of thresholding. By weighing the histogram intensity and computing the neighbouring pixels' intensity, correspondingly, the threshold in global thresholding and adaptive thresholding can be computed. When more than one TV is required to segment illuminated images, the local threshold is wielded [19]. The techniques for finding the threshold in segmentation are grounded on entropy function or optimization frameworks. Otsu, Tsallis, Masi's, and Kapur's Entropy (KE) functions are the entropy-based approaches. Particle Swarm Optimization (PSO), Spider Monkey Optimization (SMO), Differential Evolution (DE), Grey Wolf Optimization (GWO), et cetera are several optimization-centered models [8]. But, after a certain limit, these approaches have constraints; thus, an enhanced technique is required for the CIS. Superior outcomes will be attained at the segmented output image when more information about the color image is given [5]. Thus, for enriching the accuracy in image segmentation and selecting the optimal threshold, a proper technique is required by the system. Therefore, a novel methodology for CIS is proposed grounded on CLFFA optimization and RKWBS segmentation approaches.

1.1 Problem Definition

Certain negative outcomes are still required to be resolved although various methodologies have been developed for CIS grounded on heuristic algorithms. Some of such outcomes are given further,

- In the field of computer vision together with image processing, image segmentation remains challenging. Since the Region of Interest (RoI) varies for applications and the amount of extraction of RoI is tedious, there is no common approach to segment the images.
- The variation in color along with texture is dominant in color images actually. Thus, for segmenting the image into meaningful regions in a fast, robust, accurate, along with

automated way utilizing the image information like texture, color, together with intensity, an efficient image segmentation model is significant.

- When the number of thresholds is higher and color images that enclose more information are even worse, Multilevel Thresholding (MT) becomes more complicated together with time-consuming.
- As the color images comprise '3' components (Blue, Green, and Red) and every single pixel embeds dissimilar color components, the CIS becomes more complex along with challenging than the gray-scale images. Moreover, when the threshold level rises, the computational complexity enhances exponentially.
- Also, color satellite images contain fuzzy boundaries, complex backgrounds, along with poor resolution, which is tedious when compared with natural color images.
- To resolve the entire optimization issues, no approach is available. It recommends that an optimization framework may perform well for one sort of issue; also, it does not perform well to resolve various sorts of issues. Thus, creating and modifying novel optimization approaches is necessary.
- Pixel-centric segmentation frameworks are effective only for high-resolution images. It did not provide better outcomes for the low-resolution image.

To resolve these issues, the proposed model aims in developing an efficient technique for CIS grounded on an optimal TV.

The balance part of the paper is arranged as: the related works are explicated in Sect. 1.2; the proposed methodology is described in Sect. 2; the results along with discussions are elucidated in Sect. 3; finally, the paper is winded up with future work in Sect. 4.

1.2 Related Works

Zou et al. [25] presented a framework grounded on Shannon entropy difference along with Dynamic synergic entropy for automatic thresholding of image. The final segmentation threshold taken was the threshold linked with the maximum dynamic synergic entropy. The model had enhanced segmentation accuracy together with flexible adaptivity of selecting threshold. But, the guiding edge image was not computed by the model; also, the image was made inferior to other compared techniques owing to the changed contour.

Li et al. [16] developed a strategy for CIS with multi-level thresholds. The technique was grounded on the Logistic model and Chaotic map-centric Barnacles Mating Optimizer (LCBMO), which produced the high-quality optimum outcome. By the implementation of Masi entropy as the objective function, the optimal threshold was selected. The model's significance was validated by the Wilcoxon rank-sum test along with the Friedman test. However, the computational complexity made the segmentation process slower.

Chouksey and Jha [7] introduced the multiverse optimization for CIS grounded on Variational Mode Decomposition (VMD). Grounded on Tsallis along with KE functions that developed the image segmentation, the optimal threshold was determined. The outcomes proved the model's reliability regarding various computational parameters. However, owing to the stochastic characteristics of the meta-heuristic algorithm, the performance was not well at times.

Dinkar et al. [9] proffered a multilevel threshold image segmentation grounded on the Opposition-based Laplacian Equilibrium Optimizer (OB-L-EO). With the hybridization of the changing acceleration coefficient, the Opposition Based Learning (OBL) technique was applied. Otsu's interclass variance function, which achieved optimal TVs for image

segmentation, was included. Grounded on the mean value of interclass variance together with Peak Signal-to-Noise Ratio (PSNR), the OB-L-EO algorithm displayed superiority over the previous approaches. But, the model could not segment the highly illuminated images accurately.

Kandhway and Bhandari [13] established Spatial context-centric optimal multilevel energy curve thresholding for image segmentation. Here, with Otsu threshold criteria, the Cuckoo Search (CS) system was amalgamated, which executed MT over the energy curve. The numerical and visual analysis outcomes exhibited that the model was more efficient together with accurate when analogized with other techniques for color image MT. However, the salt and pepper noise present in the image could not be removed by the approach that results in reducing the output image quality.

Abdel-Basset et al. [1] propounded an Equilibrium Optimization Algorithm (EOA) for MT image segmentation issues. Owing to the capability in addressing the huge-scale issue with higher efficacy, the approach was enhanced on a meta-heuristic equilibrium system. On the Berkeley Segmentation Dataset (BSD), the experiments were executed,also, it was analogized with the seven conventional mechanisms. Concerning the metrics utilized for estimating the segmented image quality, the EOA exhibited enhanced performance. But, in Standard values along with Central Processing Unit (CPU) time for the large threshold levels, the performance was poor for some frameworks.

Bhandari et al. [3] introduced an electromagnetism-like mechanism for efficient optimal MT of image. Here, for MT-centric CIS, Renyi's entropy was amalgamated with Electromagnetism-like Mechanism Optimization (EMO). For validating the model's efficiency, experiments were conducted on the standard daily-life color images. But, when analogized with the Bat Optimization Algorithm (BOA), the Mean Square Error of the EMO was high. This affected the segmented image's quality.

Mishra and Panda [17] established a framework for CIS by the usage of Entropy-Based Thresholds. The optimal thresholds were computed with the aid of the BOA, which segmented the image. By the amalgamation of entropy-centric objective functions with BOA, the optimal TVs were attained. The superior performance of the technique on PSNR along with CPU time proved the CIS's efficacy. However, the precision of optimization was lower; hence, the results were affected.

Xu et al. [23] developed a mechanism for Unsupervised CIS with a Color-alone feature centered on RG Pulse Coupled Neural Network (CRG-PCNN). The color information was entrenched into the PCNN's linking part by a Linking Control Unit (LCN) for effective image segmentation. The experimental analysis was executed on the BSD, which exhibited that the system's segmentation accuracy was higher when analogized with the other techniques. But, when analogized with the RG-PCNN and PCNN frameworks, the technique's computational cost was high, which made the process slow.

Feng et al. [11] presented a CIS framework grounded on region salient color along with Fuzzy C-Means (FCM) approach. Convex hull theory grounded on Harris corner detection was utilized for identifying the objects in the image. For the segmentation of the background and the object, the FCM approach along with the noise correction technique was wielded on the object along with the background. The performance evaluation displayed that the system had high segmentation accuracy and lower computational costs. The model's accuracy would be affected when changes occur in the color region space owing to the hue coordinate sensitivity.

Xing and Jia [22] introduced an approach for multilevel CIS. Here, the segmentation procedure was grounded on the Gray Level Co-occurrence Matrix (GLCM); also, for the optimization of GLCM, the Levi flight Salp Swarm Algorithm (LSSA) was utilized.

Then, the Levy flight strategy enhanced the optimization of the SSA approach. The segmentation quality was evaluated through the experiments. Also, the GLCM-LSSA approach's segmentation capability was enhanced than other mechanisms. But, the GLCM could not identify the texture of the object.

Bhandari et al. [2] propounded an image segmentation model grounded on the multilevel three-dimensional (3D) Otsu function. For the simplification of the exhaustive search for the optimal threshold vector in 3D space, the Cuttlefish Algorithm (CFA)-centered 3D Otsu thresholding technique was enforced by the model. The quantitative and visual analyses were performed and established that the suggested algorithm outperformed the conventional segmentation algorithms. The quantitative and visual analyses were performed and established that the mechanism was superior to the other conventional segmentation models. However, the time complexity issue caused the model to perform slower, which is the limitation here.

Shubham and Bhandari [20] propounded a system for color image MT for natural along with satellite images centered on various entropies. Grounded on Masi entropy that handled the additive/non-extensive information concurrently, the TV was computed. When analogized with Renyi's, Tsallis, along with KE functions, the experiments conducted on the BSD showed better accuracy of color appearance after the presented model's segmentation. However, fuzzy boundaries, complex background, together with the poor resolution were included in the color satellite images. This was tedious for accurate segmentation.

Zhao et al. [24] established a system for CIS centered on hybrid schemes. Here, for the optimization of fuzzifiers and cluster centers alternatively, the Alternate PSO-centric adaptive Interval Type-2 Intuitionistic FCM clustering (A-PSO-IT2IFCM) approach was utilized. Experiments on Berkeley, as well as UC Merced Land Use datasets, exhibited that better segmentation outcomes were attained by the algorithm-determined fuzzifiers and cluster centers. However, the solution quality of the optimization of cluster centers was not good, which affected the outcomes.

Borjigin and Sahoo [4] established a scheme for CIS centered on entropy along with a 2D histogram. For RGB color image, the threshold computation model was based on Gray Level & Local-Average histogram (GLLA) and Tsallis-Havrda-Charv´at entropy. By the updation of the PSO mechanism, the optimal TV was selected. The experiments executed on the images of BSDS300 displayed better performance of the presented model than the compared schemes. But, the Global consistency error of the strategy was higher than the Shannon entropy, which affected the segmentation process's accuracy.

2 Proposed RKWBS Methodology for Image Segmentation

Since more information is provided by the color images than the gray images, one of the vital tasks in image processing is the CIS. But, the implementation of segmentation becomes a more complicated and time-consuming process when more thresholds are available. Thus, to resolve these issues, novel CLFFA and RKWBS techniques are proposed for identifying an optimal threshold. Figure 1 depicts the proposed technique's block representation.

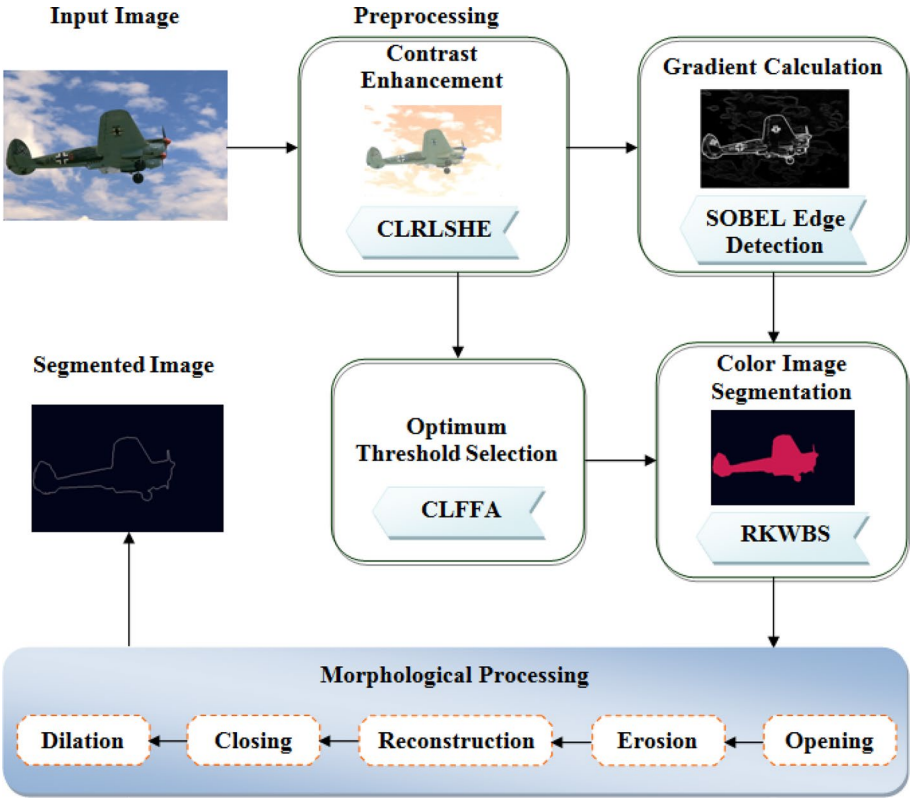

Fig. 1 Block diagram of the proposed color image segmentation process

2.1 Input Image

From the Berkeley Segmentation image dataset, the input data is collected initially. The set of color images is enclosed by the dataset, which is indicated as,

$$B_s = \{c_1, c_2, ..., c_n\} \; or \; c_i, \quad i = 1, 2, ..., n \tag{1}$$

where, B_s signifies the complete dataset and c_n symbolizes the n number of color images in the dataset.

2.2 Preprocessing

The approach utilized for cleaning the data of the input color image c_i to attain more precise results is named preprocessing. By enriching the image's contrast utilizing the CLRLSHE algorithm, the input image is preprocessed in the proposed approach. Here, for enriching the image appearance together with the CIS's outcomes, the contrast is enriched. The prevailing Contrast Limited Adaptive Histogram Equalization (CLAHE) technique has the difficulty in selecting the clip limit of the image. The modified CLAHE is termed the

CLRLSHE technique. The image quality is decreased by the improper selection of parameters. Thus, to overcome the limitation of the CLAHE algorithm, the clip limit is selected centered on the Recursive Least Square (RLS) of an image. The CLRLSHE process is examined further,

The input color image c_i is divided into several overlapping regions initially. After that, the histogram of each region is measured as,

$$H_{avg} = \frac{H_x \cdot H_y}{H_G} \tag{2}$$

wherein, the number of pixels present in x and y dimensions are denoted as H_x and H_y, the average number of pixels is indicated as H_{avg}, and the gray level regions are exhibited as H_G. Next, the contrast limit H_l was computed utilizing the clip limit value as,

$$H_{clip} = H_l \times H_{avg} \tag{3}$$

Here, H_{clip} signifies the clip limit value, and in the proposed system, H_{clip} is selected grounded on the RLS of the given image as follows,

$$H_{clip}(j) = \sum_{m=1}^{j} \varphi(j,m).(y(m))^2 \tag{4}$$

where, the variable length of each region is depicted as j, the weighting factor is signified as φ, and the estimated least squares at the time m are specified as $y(m)$. If the numbers of pixels are larger than the clip limit value, then the given pixels are clipped. Thus, a contrast-enhanced image δ_c is attained.

2.3 Gradient Calculation

Moreover, from the contrast-enhanced image, δ_c gradient magnitudes are computed grounded on Sobel edge masks. The regions of high special frequency are highlighted by the Sobel filter. This defines the object's edges present in the image. To highlight the changes in the horizontal and vertical orientations, the Sobel filter utilizes a pair of kernels. The gradient approximations are given by the kernels convolved with the input image. The gradient magnitude $|\delta_c|$ and the angle of orientation (φ) of the edge are mathematically represented as,

$$|\delta_c| = \left(\left(\delta_{c_i}\right)^2 + \left(\delta_{c_k}\right)^2 \right)^{1/2} \tag{5}$$

$$\varphi = \cos^{-1}\left(\frac{\delta_{c_i}}{\sqrt{\left(\delta_{c_i}\right)^2 + \left(\delta_{c_k}\right)^2}} \right) \tag{6}$$

where, the gradient's measurement in the horizontal and vertical orientation is denoted as $\delta_{c_i}, \delta_{c_k}$, correspondingly. Therefore, the object's edges present in the image are detected and the output image is epitomized as β_e.

2.4 Optimum Threshold Selection

By utilizing the CLFFA approach, the optimum threshold is selected as of δ_c in the proposed mechanism's third phase. The conventional Fertile Field optimization Algorithm (FFA) is grounded on the dispersal of seeds, natural factors like the wind and animals, and the plant's growth in fertile fields. In the field, finding the most fertile point is equal to finding the optimal TV. But, FFA suffers from the problems of slow and premature convergence. To resolve this issue, the Chaotic Logistic operation is adapted for updating the wind dispersion. Thus, the local optimum problem and slow or premature convergence are efficiently avoided by the proposed CLFFA technique. Moreover, the model's global detection ability is also enhanced. The steps involved in CLFFA are as follows.

Initialization All the parameters like initial seed population L_∞ (Here the population of seeds is the pixels r_a present in the image δ_c), number of plants N, number of plants that survived in all iterations a_s, and count of generated seeds in each cycle g are initialized. Then, the random distribution of seeds is given as,

$$\Delta\left(r_a\right) = \int_{\omega=1}^{L_\infty} p\left(r_{a_\omega}\right)\, dr_a \tag{7}$$

where, $\Delta()$ denotes the random seed distribution function, $p()$ denotes the probability of distribution of seeds, d denotes the integral factor, and ω denotes the random selection of seeds.

Fertility evaluation Here, the best seeds, which fell on the most fertile land, are selected. The seeds fall in the fertile region likely to grow, mature, and reproduce. Thus, finding the region with a more fertile point is equivalent to attaining the optimal value for thresholding. The segmentation accuracy is considered the seeds' fitness here. The fertility point is estimated utilizing the objective function,

$$F_{best}\left(\Delta\left(r_a\right)\right) = F_{best}\left\{\Delta\left(r_1\right), \Delta\left(r_2\right), ..., \Delta\left(r_q\right)\right\} \tag{8}$$

where, the best of the distributed seeds, which fell on the fertile land and survived, are exemplified as $F_{best}()$. The seeds are selected if $F_{best}\left(\Delta\left(r_a\right)\right) \geq TV$, where TV is the threshold value. The sorted seeds λ_s that is, the selected thresholds are denoted as,

$$\lambda_s = \left\{s_1, s_2, ..., s_o\right\} or\, s_\ell, \quad \ell = 1, 2, ..., o \tag{9}$$

wherein, s_o specify the seeds in the fertile points and capable of generating the next generation. Other seeds are discarded from the process.

Seed Generation The seeds that fell on the most fertile land have become mature and ready for pollination. When compared with the plants grown in low fertile regions, the matured plant grown in the most fertile land has more seeds. Thus, the most fertile plant that is, the optimal TV is measured as,

$$R\left(s_\ell\right) = \arg\ \max\left(s_\ell\right) = \gamma, \quad s_\ell \in \lambda_s \tag{10}$$

wherein, $R()$ indicates the fertility rate value of a plant-centered on the number of seeds produced, the attained value is regarded as the optimal TV γ. Therefore, W specifies the most fertile plant with more seeds attained. However, if the selected plant does not reach the TV, the seeds generated in the fertile plants are considered for further process as,

$$W = \{\psi_1, \psi_2, ..., \psi_u\} \; or \; \psi_z, \quad z = 1, 2, ..., u \tag{11}$$

Here, the seeds generated on the most fertile plant W is indicated as ψ_z. After that, the seeds ψ_z enter the life cycle.

Dispersion by external forces: The seeds ψ_z may fall near the most fertile plant or carry away by external forces like wind or birds. The seeds' distribution away as of the plant is represented as,

$$\ln\left(\Delta r_a\right) = \varsigma - \mu_e d \tag{12}$$

where, the count of dispersed seeds in distance d as of the mother plant is indicated as ψ_z, the seed dispersed by the wind to the position e is illustrated as μ_e, and the seeds dispersed by the birds along with animals are depicted as ζ. The wind-dispersed seeds are computed by chaotic logistics represented as,

$$\mu_e = \frac{\mu_{e+1}}{\Re\left(1 - \mu_e\right)} \tag{13}$$

where, the displaced seed position is specified as μ_{e+1}, the constant term value is indicated as $\Re$. After that, the life cycle continues by selecting the most fertile plant, which is grown on the land with the most fertility point. Lastly, the optimal TV γ is attained after a number of life cycles. The pseudocode for the proposed CLFFA system is given as,

---

Input: pixel values r_a

Output: Optimal threshold value

Begin

Initialize the parameters L_∞, N, g, a_s and maximum iteration $M_{Iteration}$

Set initial iteration $I = 0$

While $\left(I \le M_{Iteration}\right)$**do**

For each seed **do**

Evaluate the best seeds through the fertility point

If $\left(F_{best}\left(\Delta\left(r_a\right)\right) \ge TV\right)\{$

Select seed values as threshold

} **Else** {

Eliminate from life cycle

}

End If

Update most fertile plant using $\arg\max\left(s_\ell\right)$

Calculate the seeds dispersed by external force by $\ln\left(\Delta r_a\right)$

End For

End While

$I = I + 1$

Return optimal threshold value

End

2.5 Color Image Segmentation

Here, utilizing the novel RKWBS algorithm, the TV is matched with the Pixel Value (PV) of the edge detected image for the detection of only the foreground. Watershed transform is one of the gradient-centric approaches. The object border in the image is highlighted as dams and catchment basins are the segmented areas. But, unwanted contours like over-segmentation are added by the topological gradient. This can reduce the segmentation accuracy. To resolve this issue, the radial basis kernel function is wielded for measuring the distance transform instead of the Euclidean distance. The RKWBS process is given as follows,

Utilizing the distance transform, the segmentation grounded on the watershed system is measured. For image segmentation, the distance transform is amalgamated with the watershed transform. Here, to calculate the color similarity of the 2 regions, the distance transform is computed centered on the radial kernel function. The watersheds in the two regions merged are grounded on the equation,

$$\xi\left(\eta_u, \eta_{u+1}\right) = e^{\left(-\frac{\|\eta_u - \eta_{u+1}\|^2}{2\sigma^2}\right)} \tag{14}$$

where, the kernel function is indicated as $\xi()$, σ signifies the variance, which is a constant value, $\left\|\eta_u - \eta_{u+1}\right\|^2$ represents the distance betwixt the seed color pixels and the neighboring pixels corresponding to it. Here, grounded on the optimal TV, the seed PV is selected. The two regions are merged otherwise not merged if the TV $\gamma = \eta_u$. Here, the distance is the similarity to PVs. More similarity is attained if the distance is less.

The distance transformed image's complement is taken so that the light pixels present in the image display higher elevation and the dark pixels display lower elevation. The inverted distance transformed image is denoted as,

$$\upsilon = -\left[\xi\left(\eta_u, \eta_{u+1}\right)\right] \tag{15}$$

where, the output image after complementing the PVs is indicated as υ. Then, to the segmentation region, the watershed is applied. Therefore, the PVs other than the pixels in the segmented region are converted to 0, and the final watershed (i.e., segmented) is illustrated as,

$$\varepsilon = shed(\upsilon) \tag{16}$$

where, the segmented image is specified as ε, the merged region formed by the watershed transform is indicated as $shed(\upsilon)$. Hence, by utilizing the proposed RWKBS algorithm, the segmented image is attained. The pseudocode for the proposed RKWBS system is given below,

Input: Image β_e, the Threshold value
Output: Segmented image
Begin
Initialize number of basin regions ϖ, watershed, and maximum iterations $IT_{\max}$
Evaluate the basin regions
Set initial iteration it
While $(it \le IT_{\max})$ **do**
For constructing watershed **do**
Calculate distance transform based on $\xi(\eta_u, \eta_{u+1})$
Identify similarities between the two watershed regions
If $(\gamma == \eta_u)\{$
Merge similar regions
$\}$ **Else if** $(\gamma \neq \eta_u)\{$
Return without merging
$\}$
End If
End for
Construct $shed(\upsilon)$
End While
$it = it + 1$
Return segmented image
End

2.6 Morphological Processing

By morphological operations like opening, erosion, reconstruction, closing, and dilation processes, the unwanted flaws present in the segmented image are mitigated. A small template called Structuring Element (SE) is utilized by the morphology process. This is analogized with the corresponding neighbour pixels in all locations of the image. Some morphological operations check whether the SE fits in the neighbourhood, and other operations check whether SE intersects the segmented image.

Opening For eliminating the unwanted small objects in the image, the opening morphological operation is executed. Moreover, it preserves the size and shape of bigger objects present in the image. An opening operation is described as the erosion operation led by the dilation operation. The opening operation of the image ε by SE M is illustrated as,

$$\varepsilon \circ M = (\varepsilon \oplus M) \otimes M \tag{17}$$

where, the opening operator is indicated as $\circ$, the dilation and erosion operations are specified as $\oplus, \otimes$, correspondingly. Thus, the obtained image is signified as E.

Erosion By implementing the erosion process, the segmented image's boundary E is computed. The SE M is eroded with the image E as,

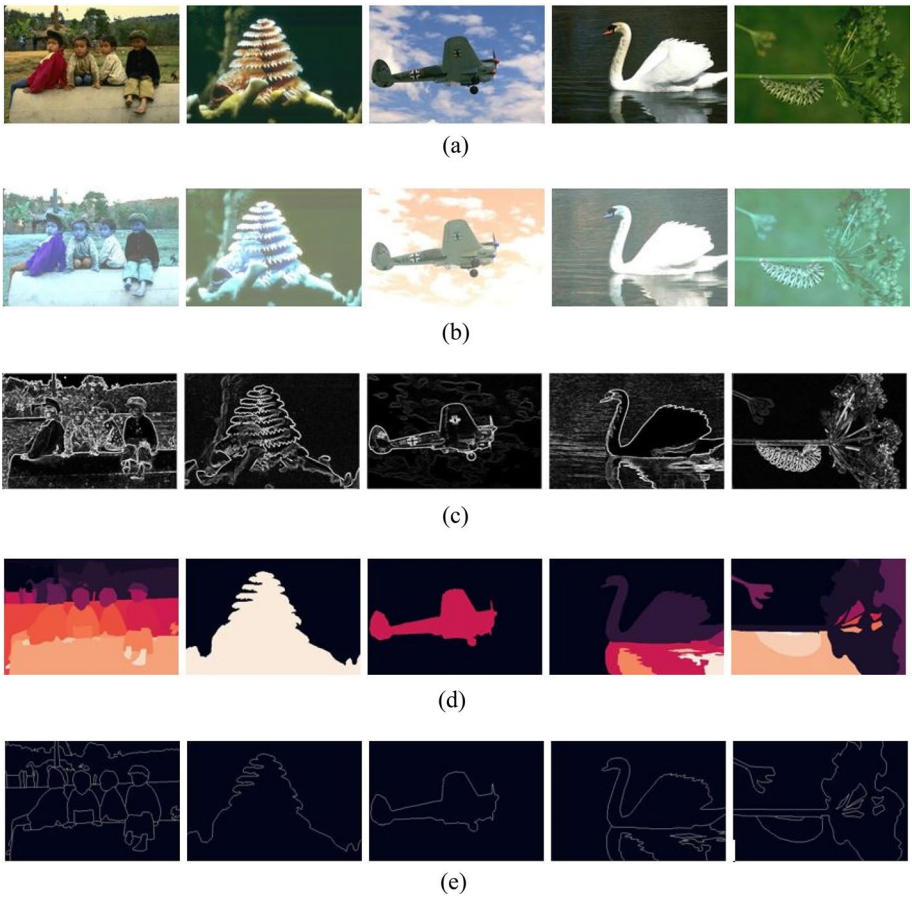

Fig. 2 Sample images outcome of the experimental analysis. (**a**) Input images. (**b**) Preprocessed images using CLRLSHE. (**c**) Sobel edge detected images. (**d**) Segmented images using the RKWBS algorithm. (**e**) Output images after morphological operations

$$(E \oplus M) = b_{image} \tag{18}$$

Here, the output binary image produced by the erosion process is specified as b_{image}. The gaps and holes betwixt the pixels are increased and the minute objects are disposed of owing to the erosion process.

Reconstruction Grounded on morphological dilation and marker image, the edge contour of the image is preserved in the reconstruction process. The process of joining pixels continues till the value change in the image is stopped here. The reconstruction operation is given as,

$$\Gamma = \left[b_{image} \otimes M\right] \cup \vartheta \tag{19}$$

where, the morphologically reconstructed image is exhibited as Γ, the reconstruction operation is specified as $\cup$, and ϑ symbolizes the marker image, which is taken by reducing the constant PVs of the image b_{image}.

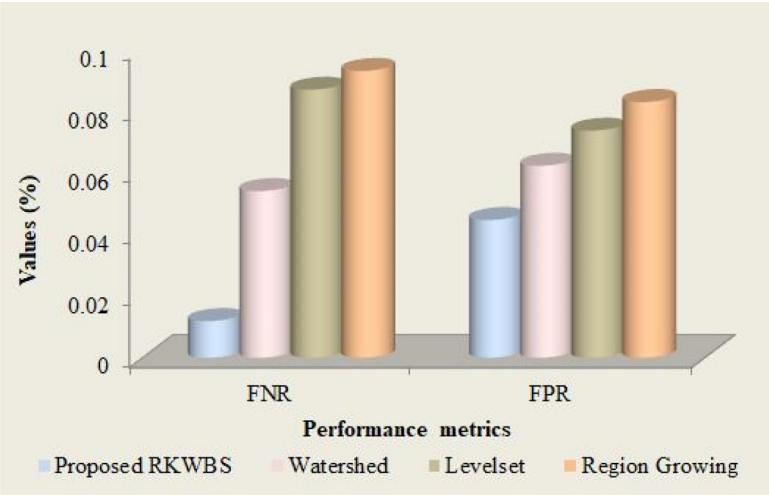

Fig. 3 FNR and FPR analysis for the proposed RKWBS algorithm

Closing The closing process is adverse to the opening process. For enhancing the color of the border of the segmented image and lightening the background present betwixt the segmented images, the closing operation is performed. The closing process is also the amalgamation of dilation and erosion operations and is epitomized as,

$$\Gamma \bullet M = (\Gamma \otimes M) \oplus M \tag{20}$$

where, the closing operator is indicated as •, which reduces the small holes present in the image. Therefore, the output image attained after the closing operation is signified as χ.

Dilation After the erosion process, dilation is performed to fill the gaps and holes, and thicken the lines. The dilation procedure applied to the image b_{image} is,

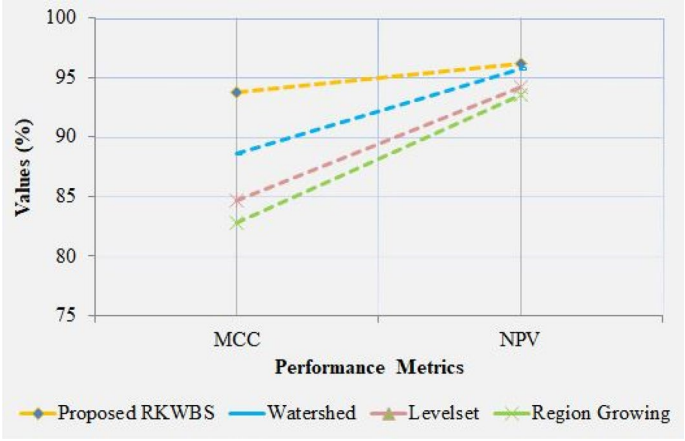

Fig. 4 MCC and NPV metrics analysis

Table 1 Comparative analysis between the proposed RKWBS and the prior techniques

Performance metrics	Proposed RKWBS	Watershed	Levelset	Region growing
Accuracy	97.7272	94.4444	93.421	91.8032
Precision	98.2142	96.1052	94.5346	93.6666
Recall	98.8023	94.5945	91.3043	90.6926
F-Measure	98.5074	93.3333	89.3617	87.8156
Specificity	98.8023	94.5945	91.3043	90.1012

$$\chi \otimes M = \Phi_{image} \tag{21}$$

Here, the dilated output image is specified as Φ_{image}. Thus, the gaps betwixt the pixels are intersected grounded on the dilation procedure. Therefore, the segmented output image is attained for the given input image centered on the RKWBS system.

3 Results and Discussion

The proposed CIS approach's performance is evaluated in this part. In the working platform of PYTHON, the experiments were executed. For the processing of the proposed mechanism, the data is gathered from the Berkeley Segmentation Dataset (BSD300). The CIS utilizing the BSD300 is displayed further (Fig. 2).

3.1 Database Description

For testing the proposed CIS technique's efficiency, the Berkeley Segmentation Dataset (BSD300) is gathered from openly available sources. 200 test images and 400 training

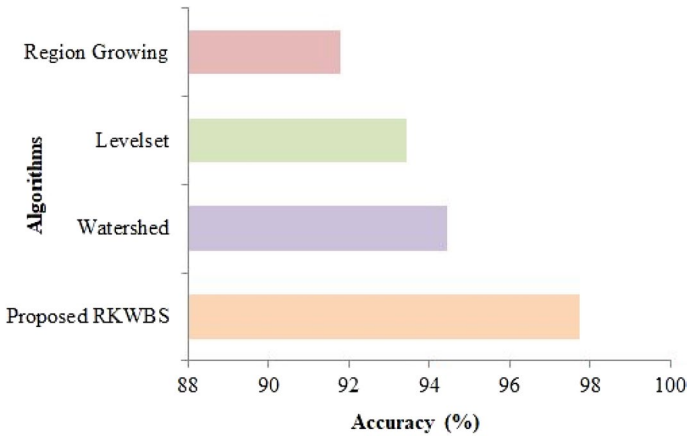

Fig. 5 Accuracy analysis

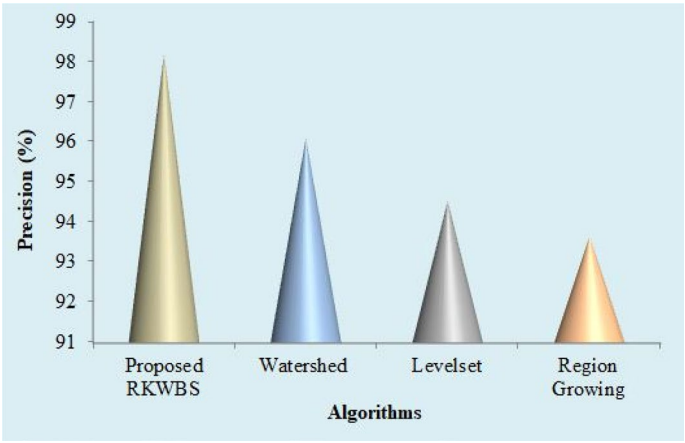

Fig. 6 Proposed RKWBS algorithm performance analysis based on Precision

images are comprised in the dataset of which 100 test images and 200 training images are color images. The test images and training images are divided into 4 and 8 classes, correspondingly with 25 images in each class.

3.2 Performance Analysis

Here, in comparison with the prevailing algorithms like Watershed, level set, and region growing, the proposed CIS algorithm RKWBS's performance is evaluated regarding precision, f-measure, computation time, False Positive Rate (FPR), Negative Predictive Value (NPV), accuracy, recall, specificity, False Negative Rate (FNR), along with Mathew's Correlation Coefficient (MCC).

Regarding FNR and FPR, the experimental analysis of the proposed RKWBS system is analogized with the prevailing algorithms like a watershed, Level set, and region growing

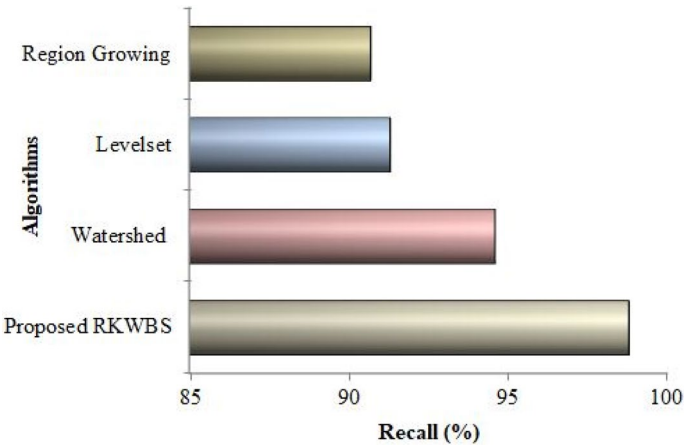

Fig. 7 Recall metric analysis

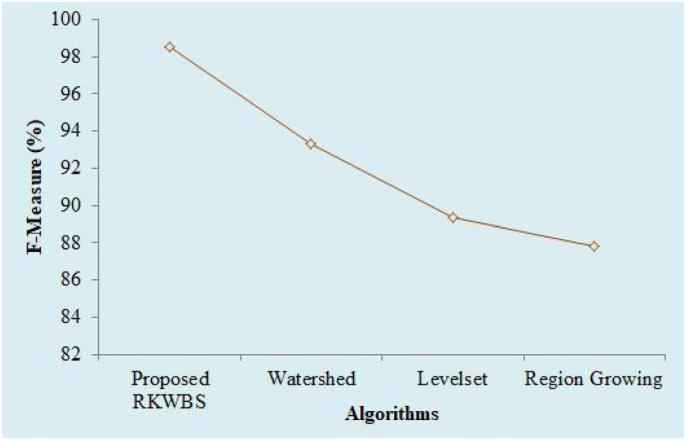

Fig. 8 Graphical representation of F-Measure analysis

in Fig. 3. The rate at which the given model failed to predict the actual positive values and actual negative values accurately is termed FPR and FNR, respectively. A better model predicts only a few false output values. Here, the FNR achieved by the proposed RKWBS is 0.0019%, which is lower than the conventional models. Moreover, 0.0446% is the FPR value attained by the proposed framework, while the prevailing techniques attain the FPR of 0.0622%, 0.0736%, and 0.829 for the watershed, level set, and region growing approaches, correspondingly. Hence, it is concluded that the output's accuracy will not be affected when utilizing the proposed RKWBS algorithm.

Figure 4 exhibits the experimental evaluation of the proposed and prevailing algorithms grounded on NPV and MCC. To verify whether the background is not segmented as an object, the NPR is computed. Thus, the prediction of NPV should be higher as possible. When analogized with the other conventional models, the NPV of the watershed algorithm is higher. But, the NPV of the proposed RKWBS is 0.49%, which is higher than the watershed technique. Moreover, the proposed system's MCC is 5.8% higher than the Watershed model and 13.18% higher than the region growing system. Higher values are produced by the MCC only when the prediction outcomes are better. Therefore,

Table 2 Experimental analysis of the proposed segmentation technique in terms of time taken for the computation

Algorithms	Computational time (ms)
Proposed RKWBS	54,345
Watershed	61,481
Levelset	74,234
Region Growing	84,746

Table 3 Comparing the accuracy performance of the proposed method with the prevailing works

Algorithms	Accuracy (%)
Proposed RKWBS	97.7272
BGGMM + FS [10]	96.68
RSCFCM [20]	82.03

in the foreground and background identification, the proposed model outperforms the conventional approaches (Table 1).

Concerning precision, f-measure, accuracy, recall, along with specificity, the proposed RKWBS's performance assessment is analogized with the conventional frameworks. The outcomes display that when analogized with the other mechanisms, lower performance is shown by the region growing approach that is, the region growing algorithm attains a specificity of 90% (approximately), which is 8.8% lower than the proposed system. Thus, from the table, it is displayed that the proposed model is superior to the prevailing approaches.

In Fig. 5, the segmentation accuracy of the proposed RKWBS system is evaluated and analogized with the prevailing models. Without any modification, the watershed algorithm attains an accuracy of 94.44%, which is 1.09% higher than the Level set approach and 2.87% higher than the region growing algorithm. However, after modification (RKWBS), the watershed model attains an accuracy of 97.7272%, which is better than the watershed segmentation alone. Thus, it is proved that the segmentation outcomes are predicted accurately by the proposed RKWBS system.

In a segmented image, to verify how many objects are segmented correctly, precision is computed. Figure 6 evaluates the precision of the proposed segmentation in comparison with the proposed system before modification and the prevailing frameworks. The precision attained by the proposed RKWBS is 2.1% higher than the conventional watershed model and 3.89% higher than the level set approach. Thus, the proposed mechanism exhibits better performance when analogized with the prevailing systems.

Figure 7 exhibits the performance evaluation of the proposed RKWBS and the prevailing techniques grounded on recall. For identifying how many objects are segmented out corresponding to the obtained output image, the recall metric is evaluated. Here, poor performance is revealed by the RG model. This means in the segmented output image, more background is segmented along with the foreground. However, a higher value of 98.80% is attained by the proposed RKWBS. This means that almost all of the foreground is segmented from the background.

Regarding F-Measure, the performance assessment of the proposed RKWBS and the conventional approaches are depicted in Fig. 8. A measure that combines precision and recall to attain the average rate of such measures is named F-measure. Better outcomes are given by a system that possesses a high f-measure value. The proposed RKWBS algorithm has the highest average rate of 98.50%, while the prevailing approaches attain 93.33%, 89.36%, and 87.81% for the watershed, Level set, and RG techniques, correspondingly, which are lower. Thus, the RKWBS algorithm gives the most accurate segmentation of objects.

The computational time analysis of the proposed RKWBS in comparison with the conventional watershed, level set, and RG algorithms is explicated in Table 2. The time taken by the system for segmenting the given input image is named computational time. Here, the proposed RKWBS algorithm runs 7136 ms faster than the watershed algorithm and 30,401 ms faster than the RG algorithm. Therefore, it is proved that the proposed RKWBS is time efficient.

The comparison of the accuracy attained in the proposed RKWBS algorithm with the prevailing Bounded Generalized Gaussian Mixture Model and Feature Selection (BGGMM + FS) algorithm and Region Salient Color and FCM (RSCFCM) algorithm are explicated in Table 3. The proposed RKWBS attains a higher accuracy (97.72%) than the other '2' prevailing frameworks. This proves the proposed RKWBS's efficacy.

4 Conclusion

This paper proposes a novel mechanism for CIS grounded on the optimal threshold selection and RKWBS algorithm. By enhancing the contrast centered on the CLRLSHE approach, the input image is pre-processed initially. Then, the CLFFA algorithm selects the optimum threshold required for image segmentation; also, the segmentation process is preceded by the proposed RKWBS technique. Experimentally, the proposed framework's performance is evaluated on the BSD300 images. The outcomes attained exhibited that the proposed RKWBS model outperformed the prevailing mechanisms. The proposed model attains a higher segmentation accuracy of 97.72%, while the prevailing approaches attain 94.44% for the watershed, 93.42% for the Level set, and 91.80% for RG, correspondingly. Moreover, when analogized with the conventional techniques, a lower run time is achieved by the proposed system. Therefore, from the overall assessment, it is proved that the proposed CIS model gives the most accurate segmentation outcome; also, it is a time-efficient model. The objects are successfully segmented here; however, it could not identify the object. Thus, for segmented object identification, an advanced system will be included with the proposed CIS model in the future.

Funding The authors have not disclosed any funding.

Declarations

Conflict of Interest The authors have no conflicts of interest to disclose.

Data Availability Enquiries about data availability should be directed to the authors.

References

1. Abdel-Basset, M., Chang, V., & Mohamed, R. (2021). A novel equilibrium optimization algorithm for multi-thresholding image segmentation problems. In *Neural computing and applications* (Vol. 33, Issue 17). Springer London. https://doi.org/10.1007/s00521-020-04820-y
2. Bhandari, A. K., Kumar, I. V., & Srinivas, K. (2020). Cuttlefish algorithm-based multilevel 3-D Otsu function for color image segmentation. *IEEE Transactions on Instrumentation and Measurement, 69*(5), 1871–1880. https://doi.org/10.1109/TIM.2019.2922516
3. Bhandari, A. K., Singh, N., & Shubham, S. (2019). An efficient optimal multilevel image thresholding with electromagnetism-like mechanism. *Multimedia Tools and Applications, 78*(24), 35733–35788. https://doi.org/10.1007/s11042-019-08195-8
4. Borjigin, S., & Sahoo, P. K. (2019). Color image segmentation based on multi-level Tsallis–Havrda–Charvát entropy and 2D histogram using PSO algorithms. *Pattern Recognition, 92*, 107–118. https://doi.org/10.1016/j.patcog.2019.03.011
5. Channoufi, I., Bourouis, S., Bouguila, N., & Hamrouni, K.(2018). Color image segmentation with bounded generalized Gaussian mixture model and feature selection. In *4th International conference on advanced technologies for signal and image processing* (pp. 1–6). https://doi.org/10.1109/ATSIP.2018.8364459
6. Chen, J., Zheng, H., Lin, X., Wu, Y., & Su, M. (2018). A novel image segmentation method based on fast density clustering algorithm. *Engineering Applications of Artificial Intelligence, 73*, 92–110. https://doi.org/10.1016/j.engappai.2018.04.023
7. Chouksey, M., & Jha, R. K. (2021). A multiverse optimization based colour image segmentation using variational mode decomposition. *Expert Systems with Applications, 171*, 114587. https://doi.org/10.1016/j.eswa.2021.114587

8. De, S., Dey, S., Debnath, S., & Deb, A. (2020). A new Modified Red Deer Algorithm for multi-level image thresholding. In *Proceedings – 2020 5th international conference on research in computational intelligence and communication networks, ICRCICN 2020* (pp. 105–111). https://doi.org/10.1109/ICRCICN50933.2020.9296166
9. Dinkar, S. K., Deep, K., Mirjalili, S., & Thapliyal, S. (2021). Opposition-based Laplacian equilibrium optimizer with application in image segmentation using multilevel thresholding. *Expert Systems with Applications, 174*, 114766. https://doi.org/10.1016/j.eswa.2021.114766
10. Farshi, T. R., Drake, J. H., & Özcan, E. (2020). A multimodal particle swarm optimization-based approach for image segmentation. *Expert Systems with Applications*, *149*. https://doi.org/10.1016/j.eswa.2020.113233
11. Feng, L., Li, H., Gao, Y., & Zhang, Y. (2020). A color image segmentation method based on region salient color and fuzzy C-means algorithm. *Circuits, Systems, and Signal Processing, 39*(2), 586–610. https://doi.org/10.1007/s00034-019-01126-w
12. García-Lamont, F., Cervantes, J., López-Chau, A., & Ruiz-Castilla, S. (2020). Color image segmentation using saturated RGB colors and decoupling the intensity from the hue. *Multimedia Tools and Applications, 79*(1–2), 1555–1584. https://doi.org/10.1007/s11042-019-08278-6
13. Kandhway, P., & Bhandari, A. K. (2020). Spatial context-based optimal multilevel energy curve thresholding for image segmentation using soft computing techniques. In *Neural computing and applications* (Vol. 32, Issue 13). Springer London. https://doi.org/10.1007/s00521-019-04381-9
14. Khan, A., ur Rehman, Z., Jaffar, M. A., Ullah, J., Din, A., Ali, A., & Ullah, N. (2019). Color image segmentation using genetic algorithm with aggregation-based clustering validity index (CVI). *Signal, Image and Video Processing, 13*(5), 833–841. https://doi.org/10.1007/s11760-019-01419-2
15. Lang, C., & Jia, H. (2019). Kapur's entropy for color image segmentation based on a hybrid whale optimization algorithm. *Entropy, 21*(3), 318. https://doi.org/10.3390/e21030318
16. Li, H., Zheng, G., Sun, K., Jiang, Z., Li, Y., & Jia, H. (2020). A logistic chaotic barnacles mating optimizer with masi entropy for color image multilevel thresholding segmentation. *IEEE Access, 8*, 213130–213153. https://doi.org/10.1109/ACCESS.2020.3040177
17. Mishra, S., & Panda, M. (2018). Bat algorithm for multilevel colour image segmentation using entropy-based thresholding. *Arabian Journal for Science and Engineering, 43*(12), 7285–7314. https://doi.org/10.1007/s13369-017-3017-x
18. Nguyen, T. K., KhoaCoustaty, M., Jean Loup, G. (2018). A new image segmentation approach based on the louvain algorithm. In *International workshop on content-based multimedia indexing* (pp. 1–6). https://doi.org/10.1109/CBMI.2018.8516531
19. Phornphatcharaphong, W., & Eua-Anant, N. (2020). Edge-based color image segmentation using particle motion in a vector image field derived from local color distance images. *Journal of Imaging, 6*(7), 1–19. https://doi.org/10.3390/jimaging6070072
20. Shubham, S., & Bhandari, A. K. (2019). A generalized Masi entropy based efficient multilevel thresholding method for color image segmentation. *Multimedia Tools and Applications, 78*(12), 17197–17238. https://doi.org/10.1007/s11042-018-7034-x
21. Xing, Z. (2020). An improved emperor penguin optimization based multilevel thresholding for color image segmentation. *Knowledge-Based Systems, 194*, 105570. https://doi.org/10.1016/j.knosys.2020.105570
22. Xing, Z., & Jia, H. (2019). Multilevel color image segmentation based on GLCM and Improved salp swarm algorithm. *IEEE Access, 7*, 37672–37690. https://doi.org/10.1109/ACCESS.2019.2904511
23. Xu, G., Li, X., Lei, B., & Lv, K. (2018). Unsupervised color image segmentation with color-alone feature using region growing pulse coupled neural network. *Neurocomputing, 306*, 1–16. https://doi.org/10.1016/j.neucom.2018.04.010
24. Zhao, F., Chen, Y., Liu, H., & Fan, J. (2019). Alternate PSO-based adaptive interval type-2 intuitionistic fuzzy C-means clustering algorithm for color image segmentation. *IEEE Access, 7*(c), 64028–64039. https://doi.org/10.1109/ACCESS.2019.2916894
25. Zou, Y., Zhang, J., Upadhyay, M., Sun, S., & Jiang, T. (2020). Automatic image thresholding based on Shannon entropy difference and dynamic synergic entropy. *IEEE Access, 8*, 171218–171239. https://doi.org/10.1109/ACCESS.2020.3024718

Publisher's Note Springer Nature remains neutral with regard to jurisdictional claims in published maps and institutional affiliations.

Springer Nature or its licensor (e.g. a society or other partner) holds exclusive rights to this article under a publishing agreement with the author(s) or other rightsholder(s); author self-archiving of the accepted manuscript version of this article is solely governed by the terms of such publishing agreement and applicable law.

Chandana Kumari I am a research scholar in Birla Institute of Technology. I am working for the development of mathematical model for the Image Segmentation and Optimizations. I am a lecturer in Computer science and Engineering in Al-Kabir Polytechnic. My Institution is the best in the Jharkhand state. I thrive on challenges and explore new ideas to work on that in the field of academics

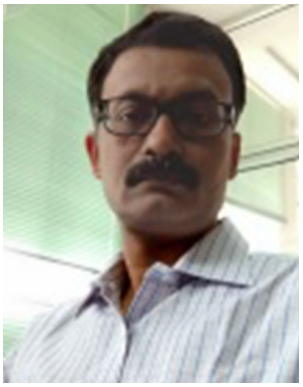

Abhijit Mustafi did his Master of Computer Applications from the University of North Bengal, India, and his Ph.D. from the Birla Institute of Technology, Mesra, India. His Doctoral thesis was in the domain of Blind Source Image Separation using the fractional Fourier transform. His current research interests include Text mining, Image Processing, and Deep Learning. He has more than ten journal publications and conference proceedings to his credit. Dr. Mustafi is currently with the BIT Mesra, India, associated with the Department of CSE.